Soft Matter

RSC Publishing

PAPER

View Article Online
View Journal | View Issue

Cite this: *Soft Matter*, 2013, **9**, 1344

Dynamics of poly-nipam chains in competition with surfactants at liquid interfaces: from thermoresponsive interfacial rheology to foams

Reine-Marie Guillermic† and Arnaud Saint-Jalmes

Received 18th July 2012
Accepted 13th November 2012

DOI: 10.1039/c2sm26666k

www.rsc.org/softmatter

We report results on the interfacial viscoelasticity and foaming of solutions of a thermoresponsive polymer (poly-*n*-isopropylacrylamide) with and without added surfactants, and as a function of temperature. With pure polymer solution, a clear transition is evidenced: both interfacial shear and dilational rheology shift from a fluid-like to a solid-like behavior at a well-defined temperature. The high temperature regime shows that the layer shares many features with soft glassy systems. At all temperatures, the foaming is low and the foam produced is unstable. Adding a surfactant not only helps to foam and to stabilize the foam, but also removes the thermal responsivity of the interfacial viscoelasticity. Under the conditions used here, we observe that the surfactant concentration threshold for altering the high temperature interfacial viscoelasticity is low, and is of the order of 1% of the surfactant critical micelle concentration. It turns out to be very different from critical values for the polymer–surfactant association found previously by structural studies (in bulk and at interface), and also below the threshold value required to stabilize the foam.

I Introduction

Small molecular weight surfactants are widely used because they easily adsorb on gas–liquid or liquid–liquid interfaces. Once with large amounts of adsorbed surfactants, a fluid interface is significantly modified: a smaller surface tension is obtained, and the interface can acquire an electric charge or can develop 2D viscoelastic features. Because surfactants modify the interfaces in such ways, they are crucial for producing and stabilizing all types of liquid dispersions (like foams and emulsions) in various applications and fields like cosmetics, detergency, or in the food industry.[1–3] Surfactants not only help for the formation of a liquid dispersion, but many macroscopic properties of such dispersions are directly linked to the interfacial structural and dynamical properties, driven by the chemical formulation at the interfaces.[4,5]

Beside dispersed materials, it has recently emerged that the dynamics of processes involving single liquid films or free interfaces are controlled by the coupling between bulk and interfacial hydrodynamics. For instance, in the cases of plate or fiber coating[6,7] or for the slip of bubbles on walls,[8] it turns out that there is strong coupling between the interfacial and bulk rheology, and that the dynamics at interfaces can have an impact on the final macroscopic features. To rationalize these effects, non-dimensional numbers are used and identified as control parameters, eventually including purely 2D characteristics.[6,7,9,10] Altogether, it is clearly emerging that the rheology of liquid interfaces, controlled by the adsorbed species, can play a key role in many multiphasic materials and applications.

In parallel to the small weight surfactants used primarily in detergents, dishwashing liquids or shampoos, some polymers can also adsorb at interfaces. Such amphiphilic polymers can be either natural, like proteins,[11,12] or synthetic ones. They act similarly as surfactants on interfacial properties. However, adsorbed polymer layers offer more complex features. While surfactants can basically only make monolayers, various configurations of adsorption are found with polymers (loops, mushrooms).[13] The adsorbed layer can then have non-trivial longitudinal and transverse density profiles. Moreover, adsorption and desorption timescales of polymers are much longer than for surfactants. As a consequence, surface concentration gradients can easily be produced under interfacial deformation. In fact, from this dynamical point of view, the polymeric layer can actually develop high interfacial viscoelasticity, well above what is obtained for small weight surfactants. This is especially true in terms of interfacial shear viscoelasticity.[14] Under shear, the shape of the interface is modified, but not its area: small surfactants usually do not provide elastic response to such deformations, while a polymeric layer can, because of chain entanglements or multi-site adsorption.

Understanding the links between the polymer intrinsic features (like its mass, rigidity or solvent affinity) and the interfacial dynamical properties is difficult and a clear

Institut de Physique de Rennes, UMR 6251 CNRS/Université Rennes 1, 35042 Rennes Cedex, France

† Present address: Department of Physics and Astronomy, University of Manitoba, Winnipeg, Manitoba R3T 2N2, Canada.

identification of the microscopic key parameters which control the interfacial rheology is still missing. This makes it even more speculative to draw links towards higher scales, *i.e.* between the polymer intrinsic properties, the dynamical interfacial properties and the macroscopic processes or materials. Approaches based on comparing results obtained with different polymers are tricky, as often too many parameters may change simultaneously.

To make progress on these issues, a possible approach consists of investigating model single-component systems, whose properties can be modified in controlled ways. Poly-*n*-isopropylacrylamide, abbreviated as pnipam in the following, is a water-soluble polymer having a lower critical solubility temperature (reported at $T_{LCST} = 32.5 \pm 1$ °C). This means that, for any pnipam solution, there is a critical temperature T_c below which water is a good solvent, while the pnipam chains collapse above T_c (ref. 15–19) and this transition is reversible. For pnipam, the value of T_c is almost constant in a large range of chain molecular mass and concentration, and practically identical to its lower value T_{LCST}. Moreover, this polymer is surface active and adsorbs at interfaces.[20–26] Interestingly, these structural results showed that different interfacial configurations are obtained by tuning the temperature. More precisely, significant and reversible changes of thickness and density are obtained from below and above T_c.[24] A transition from a low density layer to a thick and dense layer is obtained just by tuning the temperature, keeping the chemical formulation of the polymer constant. At interfaces, much less work has been done on the interfacial viscoelasticity, and it is still not clear how the interfacial rheology depends on temperature. A previous work on the shear viscoelasticity showed that there is also a strong dependence with temperature.[27] But there are still many missing points to understand this whole interfacial dynamics and its dependence on temperature; in particular, concerning the effect of temperature on the response to dilational perturbations.

In fact, a full characterization of the rheology of pnipam-covered interfaces is required to determine if formulations based on pnipam could actually be efficient routes to obtain widely tunable interfacial viscoelasticity (just by changing T). Indeed, having such a system would help to carefully determine the links not only between polymer properties and viscoelasticity but also between this viscoelasticity and macroscopic features. In that spirit, ideal macroscopic systems, in which properties are dependent on interfacial rheology, are dispersions like foams and emulsions. If one wants to better understand these links between the interfacial viscoelasticity and the macroscopic dispersions, it is also important to know if pnipam chains can be efficient stabilizers of dispersions, how a surfactant and this polymer interact at interfaces and if a thermal responsivity of the interfaces can be transposed to the 3D hierarchical structure of a dispersion. On all these aspects, in particular on the interaction of pnipam with surfactants as a function of temperature, it is also necessary to check how consistent are the studies in the bulk,[16,17,28,29] the static studies at interfaces,[30–33] and the rheological properties at interfaces. Moreover, understanding the interaction between surfactants and polymers, in the bulk and at the interface, for good and bad solvent conditions, is also a fundamental and important issue.

Here, we first report a new set of results on the viscoelasticity of interfaces covered with pnipam, and secondly on foams containing pnipam. We show how dilational viscoelasticity indeed also drastically changes with temperature. We also implement previous works on shear response, using here a different method allowing us to investigate the rheology of the elastic regime at high temperature. We also present the results of the addition of a surfactant on these interfacial and foam properties. Strong effects of the surfactant are observed: we show that the surfactant concentration threshold values for modifying interfaces and foams are different, and depend on temperature.

II Experimental information: materials and methods

A Chemicals

Poly-*n*-isopropylacrylamide (pnipam) was purchased from Sigma-Aldrich, and has a mean molecular mass of 25 000 g mol^{-1}. Keeping in mind that we want to investigate foaming, we have chosen a rather small M_w, and will work with concentrations c_p up to 10 g L^{-1}. We used sodium dodecyl sulfate (SDS) as a surfactant, which was also purchased from Sigma-Aldrich. All the solutions were prepared with Millipore water. The polymer is poured into water and the solution was stirred until complete dissolution. Surfactants were added afterward, and the solution was stirred again.

B Interfacial tension

The interfacial tension γ is measured using a pendant drop tensiometer. In the static mode of the tensiometer, a millimetric liquid drop of controlled volume is formed at the tip of a syringe. By image analysis, the interfacial tension is measured, solving the Laplace equation describing mechanical equilibrium under capillary and gravity forces.

C Interfacial dilatational viscoelasticity

The mechanical response to compression–dilatation of the interfaces is studied by the oscillatory drop method. The same setup as for the interfacial tension measurement is used, but in a dynamic mode. In that case, accurate sinusoidal oscillations of the volume are performed, corresponding to controlled compression–dilatation of the interfacial area.[34] Then by monitoring the in-phase and out-of-phase response of the surface tension, the dilatational elastic and viscous moduli, E_i' and E_i'', can be determined (E_i, being the complex modulus: $E_i = E_i' + iE_i''$). Note that compression–dilatation solicitations mostly reflect the exchange of molecules between the bulk and the interface.

D Interfacial shear viscoelasticity

A bi-conical setup mounted on a rheometer (Anton Paar MCR 301) is used to measure the interfacial shear rheology. The interface is sheared between the rotating inner bicone and the

outer container wall.[35,36] All the usual 3D rheological measurements can then be transposed in 2D. In particular, oscillatory measurements like amplitude- or frequency-sweeps can be performed. Taking into account the corrections from the bulk,[35,36] one can then derive the interfacial storage $G_i^{'}$ and loss moduli $G_i^{''}$ as a function of the strain amplitude τ or frequency f. In practice, 100 mL of solution are required to fill the experimental cup. Once this cup is filled, setting up the instruments requires about 15 minutes before running the first measurement. In contrast with dilational solicitations, shear deformation mostly reflects the interactions and flows within the interface (interfacial area does not change, only its shape).

E Temperature measurements and experimental ramping for interfacial studies

We used different types of ramps for changing the temperature. Experiments are either performed with a continuous rate dT/dt, or by steps of ΔT with variable waiting times at a given T, or by creating the interface at any given temperature T. For the pendant drop apparatus, the temperature is set by a water circulation thermalizing a transparent cell in which the syringe tip and the drop are placed. A temperature probe measures the temperature close to the pendant drop. For a better precision, we also used an IR camera for taking pictures of the drop, and providing a direct temperature measurement. The interfacial shear cell is thermalized by high precision Peltier devices; here also, the IR camera is complementarily used to measure the temperature of the interface.

F Bulk shear viscoelasticity

We used the same rheometer (Anton Paar MCR 301) as for interfacial shear, to measure the bulk rheological properties. As the viscosities are actually close to that of pure water, a double-gap Couette geometry, well-suited for low viscosities, is chosen.

G Foam studies

The experimental measurements on foams are made in a transparent rectangular column of section 8 cm and height 30 cm. At the bottom, gas is injected at various controlled flow rates through glass frits of controlled porosities. All together, changing the frit porosity and the gas rate allows us to test the foamability of the solution and stability of the foam as a function of the bubble diameter, and liquid fraction. On opposite sides of the cell are incrusted electrodes allowing us to measure the local liquid fraction as a function of time, thanks to a calibration relating electrical conductivity and liquid fraction.[37] The solution foamability is deduced by comparing the rate of gas injection and foam production, indicating how efficient is the gas incorporation in the foam. The subsequent stability of the foam is monitored by the electrical measurements and by taking close-up pictures. The pnipam-based solutions are introduced at the desired temperature inside the column, and the bubbling starts immediately.

III Results for pure pnipam solutions

A Interfacial properties

We first report how the equilibrium surface tension evolves with temperature. Results of surface tension and temperature as a function of time, during a ramp is shown in Fig. 1 (concentration of pnipam $c_p = 10$ g L^{-1}). The surface tension first decreases as T increases, but at $T_1 = 34$ °C, two features occur simultaneously: the surface tension saturates becoming almost independent of T, and the pendant drop becomes opaque. This is fully reversible: decreasing the temperature, the drop gets transparent and the surface tension increases again once below the same threshold T_1. Getting rid of time, the results of such measurements as a function of the temperature are shown in the inset of Fig. 1, evidencing a clear kink and change of regime at this well defined T_1. Quantitatively, the range of interfacial tensions measured is around 40 mN m^{-1}: this is significantly below the value of pure water, meaning that a large amount of matter is actually adsorbed.

To investigate the dilational viscoelasticity, the pendant drop is put under sinusoidal oscillations of its area. A first way of showing a temperature dependent viscoelasticity is shown in Fig. 2. Here, a similar temperature ramp is performed as in Fig. 1, together with small oscillations of the drop area (amplitude of 1%, frequency = 0.2 Hz). When T passes over a critical value, we observe strong surface tension variations, in phase with the area solicitations. In this high temperature range, the surface tension becomes dependent on the interfacial area: γ decreases under compression, and inversely. For each temperature, we performed such oscillatory measurements, from which the interfacial elastic and viscous part are derived. It turns out that – when surface tension variations are observed – the elastic part remains always the dominant contribution. In the following, we only consider the amplitude of E_i, as $E_i \approx E_i^{'} \gg E_i^{''}$. In Fig. 3, we show how this dilatational modulus evolves with temperature: there is nothing measurable up to $T_2 = 34 \pm 0.5$ °C, and a clear increase above. Note that E_i reaches values of 50–60 mN m^{-1}, corresponding to the range of high values when compared to the literature and meaning highly elastic interfaces. Note also that E_i tends to saturate with

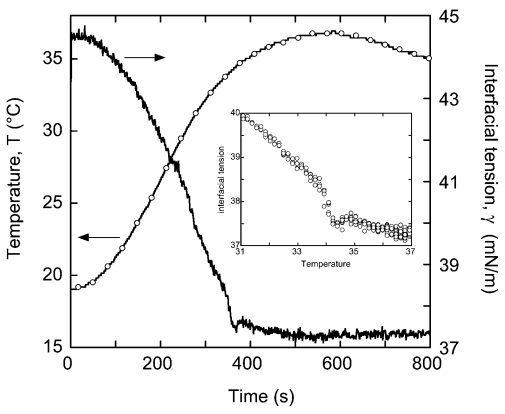

Fig. 1 Interfacial tension of a pnipam solution ($c_p = 10$ g L^{-1}) as a function of time, during a temperature ramp. Inset: interfacial tension *vs.* temperature T.

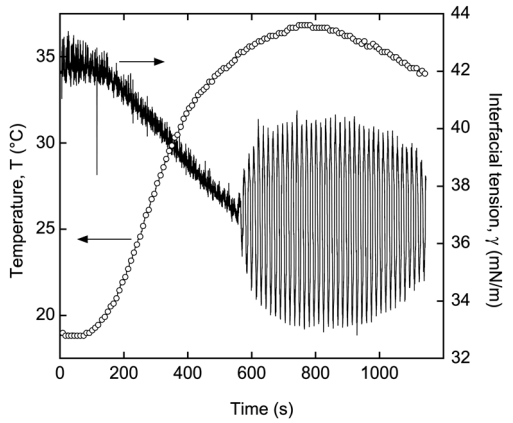

Fig. 2 Interfacial tension of a pnipam solution ($c_p = 10$ g L^{-1}) as a function of time, during a temperature ramp, together with volumetric oscillations of the pendant drop.

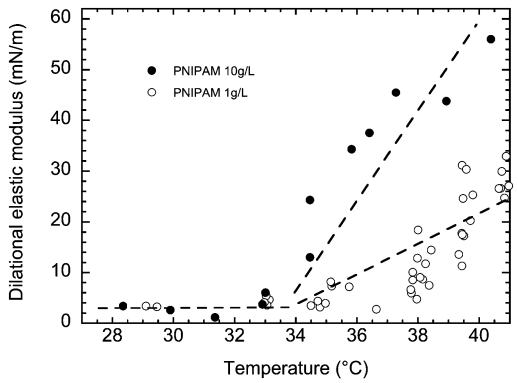

Fig. 3 Interfacial compression modulus as a function of temperature T, for two pnipam concentrations.

temperature. Fig. 3 also shows the effect of the pnipam concentration: for 1 g L^{-1}, the same features are observed, with a same critical temperature, but with smaller elasticity values. We also investigated the response to different frequencies and amplitudes of oscillations: no significant variations have been found within the range which can be investigated by our device (frequencies limited to the range 0.05 Hz to 0.5 Hz).

Another important aspect to investigate is the effect of the experimental heating protocol (meaning various rates of change of temperature). First, the temperature is increased step by step, but with various step sizes and waiting times at each step. It turns out that these different heating sequences provide the same results. Secondly, by heating the solution first and creating the interface at any given temperature, we have measured the same qualitative features as in Fig. 2, but with elasticity values typically lowered by 10 to 30%.

Together with dilational measurements, we performed shear viscoelasticity measurements, more precisely amplitude sweeps, at different T. In such experiments the frequency is fixed at $f = 0.2$ Hz, the amplitude τ is varied from 0.2% to 10% and we measure the interfacial shear elastic and viscous moduli. Results are shown in Fig. 4. For T below a transition

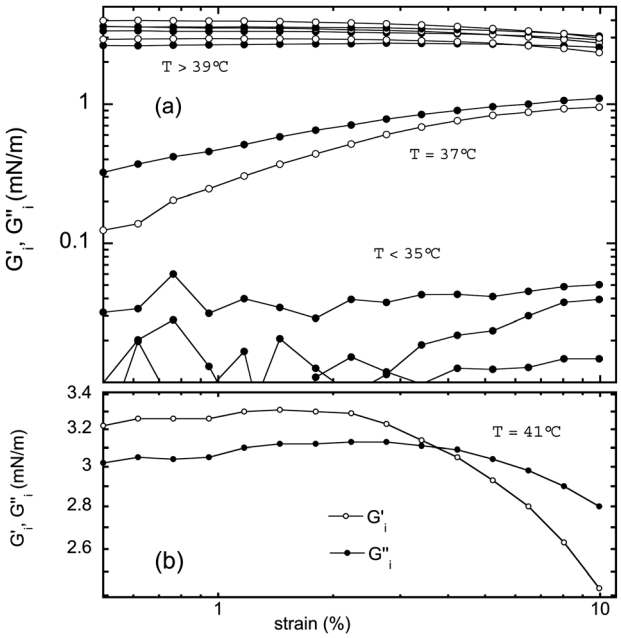

Fig. 4 (a) Interfacial shear moduli, $G_i^{'}$ and $G_i^{''}$, as a function of amplitude strain τ for different temperatures. (b) Behavior in the high temperature range, illustrated by the results for $T = 41$ °C. At all temperatures, open symbols are for $G_i^{'}$ and closed symbols for $G_i^{''}$.

value T_3, only a viscous contribution is measured, corresponding to fluid-like interfaces, and at the limit of resolution of the apparatus. With T, both $G_i^{'}$ and $G_i^{''}$ increase, with $G_i^{'}$ eventually becoming dominant. In Fig. 4a, one can see the results for $T = 37$ °C, corresponding to $G_i^{'} \approx G_i^{''}$. While Fig. 4a shows the changes of orders of magnitude with T, Fig. 4b is a close-up in the range of high T. A plateau of $G_i^{'}$ is observed at low strain τ where $G_i^{'} > G_i^{''}$, whereas $G_i^{''} > G_i^{'}$ above a yield strain τ_c of 2–4%. From these data, we can plot in Fig. 5 $G_i^{'}$ and $G_i^{''}$ for a given frequency and strain ($f = 0.2$ Hz, $\tau = 1\%$) as a function of temperature. We recover trends similar to those for dilational measurements, with almost no response at low temperature, and strong increase of the moduli above a critical temperature $T_3 = 33.5 \pm 1$ °C.

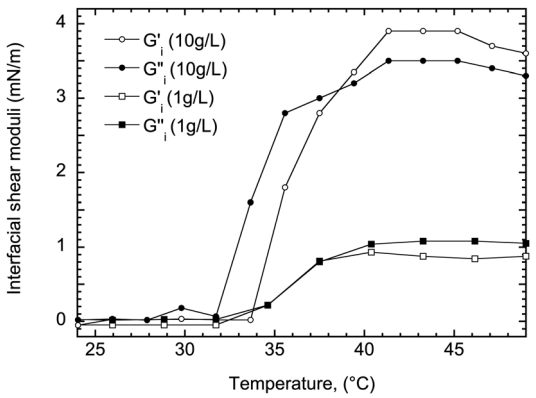

Fig. 5 Evolution of $G_i^{''}$ and $G_i^{''}$ as a function of T, for two polymer concentrations. Data are collected for a given frequency and strain: $f = 0.2$ Hz and $\tau = 1\%$.

Concerning the role of the protocol, similar trends to what is found for dilational rheology are obtained: we observe no effect of the heating protocol, except in the case where the interface is produced directly from an already hot solution at $T > T_3$ which leads to smaller values of the moduli (typically 20–30%). As well, for the effect of the concentration of polymer, we also plotted the results obtained for $c_p = 1$ g L^{-1} in Fig. 5. A change above T_3 is also observed, but here the increase of the moduli is smaller than for $c_p = 10$ g L^{-1} and the elastic part never dominates.

The yielding features, with a critical strain τ_c, seen in the regime of high temperature deserved more investigation. We also performed a specific type of oscillatory measurements, done at constant shear rate $\dot{\tau}$: strain and frequency are simultaneously and inversely varied so that their product $\dot{\tau} = \tau \times f$ remains constant. Recent results showed that performing sweeps of frequencies at constant shear rates reveals characteristics, which are hidden in usual oscillatory tests.[38–40] Fig. 6 shows the results for a fixed shear rate of 10^{-2} s^{-1}: a crossover frequency F_c is revealed under this oscillatory protocol, separating viscous and elastic dominated regimes. For this shear rate, if the interface is oscillated slowly enough ($f < F_c$), the stress is always relaxed so that the interface responds viscously. Inversely for $f > F_c$ stresses can be stored which mean that the interface has an elastic behavior. The same types of curves are then recovered at all constant shear rate measurements, with always a characteristic frequency F_c. In the inset of Fig. 6, we have plotted the evolution of F_c as a function of the shear rate. The data can be adjusted by a functional form:[38–40]

$$F_c = F_{c0} + \alpha\dot{\tau}^{\beta} \quad (1)$$

with $\alpha = 3$ and $\beta = 0.8 \pm 0.1$, and $F_{c0} = 0.09 \pm 0.04$ Hz being the constant in the limit of low shear rates. We will come back to the meaning of these data, in terms of soft glassy disordered materials in Section V.

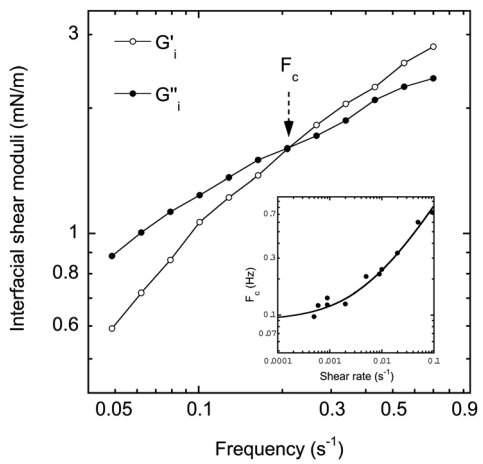

Fig. 6 Results of oscillatory measurements at a constant shear rate $\dot{\tau} = 10^{-2}$ s^{-1}, for $T = 41$ °C. At all $\dot{\tau}$, a crossover frequency F_c can be extracted and the evolution of F_c with $\dot{\tau}$ is reported in the inset.

B Bulk, foaming and stability

Concerning the bulk properties, the first result is that the bulk viscosity is basically independent of T and of the shear rate: only a small increase up to 1.7 ± 0.3 mPa s close to the temperature $T_4 = 34$ °C whereas the viscosity is equal to 1.25 ± 0.12 mPa s in the rest of the temperature range.

The data are collected for a gas injection through a frit of porosity 3 (*i.e.* 40–60 microns pore size), experimentally leading to bubbles of mean diameter d_{theo} = 400–500 microns for solutions having a maximal foamability (such as a surfactant solution above the cmc). Fig. 7 illustrates the typical results on this foaming and the subsequent foam stability of a solution of pnipam at 10 g L^{-1}. We have plotted the local liquid fraction, at a fixed height in the column, corresponding to 20 cm above the top of the liquid solution. In parallel, we have added pictures of the foam at this location.

At a continuous low gas flow rate (0.1 L min^{-1}), extremely dry foams are produced ($\varepsilon < 0.1\%$) with larger bubbles than expected for good foaming, and only a final amount of foam is produced (of the order of 10 cm): because of its dryness, the foam collapses at a rate similar to its production rate. In contrast, at the highest flow rates (1 L min^{-1} and higher), any required foam volume can be made, but still with bubbles at least two times bigger than d_{theo} and always corresponding to liquid fractions $\varepsilon \approx 0.3$. The initial bubble size and the liquid fraction cannot be controlled, meaning that the foam already evolves and collapses even during the fastest production process.

Once the production is stopped, $t = t_0$, a total foam collapse occurs within the first minutes: the bubble diameter grows everywhere and large holes are created, as shown by the pictures in Fig. 7. As a direct consequence, the local liquid fraction drops within tens of seconds; this decay is at least ten times faster than for a foam with no bubble coalescence (for a same initial

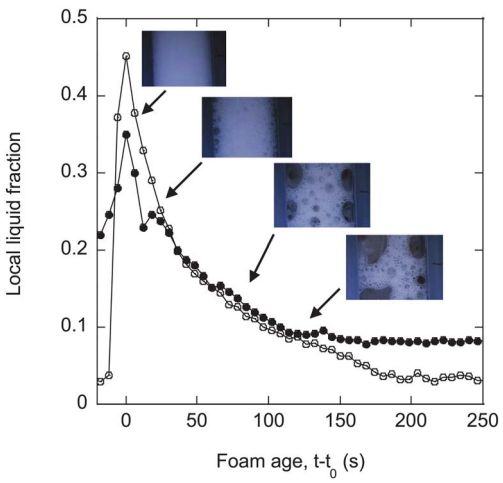

Fig. 7 Results of the foaming of pure pnipam solution and of the stability of the foams. The liquid fraction is given as a function of the foam age $t - t_0$, where t_0 corresponds to the end of foam production. Foam pictures are added at various aging times, illustrating the rapid collapse of the foam. The two curves correspond to two temperatures (open symbols: 22 °C and closed symbols: 38 °C).

bubble diameter and liquid fraction). As for a given pair of electrodes one determines the local amount of liquid, the results for a given height depends on the amount of coalescence and of the occurrence of holes at this height. Nevertheless, the most important features – large holes occurring rapidly and randomly within the foam, leading to sharp decrease of the liquid fraction – are recovered for all samples, and these qualitative trends are monitored at all heights. Experiments can also be done with solutions pre-heated at any given T. We have found these same features at all temperatures (Fig. 7): the foam stability remains poor and it is impossible to detect significant variations with temperature. Differences as in Fig. 7 are not relevant and only reflect that, at this given foam height, more coalescence occurred in the experiment done at $T = 22$ °C than at $T = 38$ °C.

We can then summarized that – whatever the pure-pnipam solution temperature – this solution has first a medium foamability because some foams can be produced, but only under strong energy input and with high liquid fractions ($\varepsilon > 0.25$), and secondly the foams have then low stability against film ruptures and coalescence. A consequence of this low stability at all temperatures is that it is impossible to stabilize the foam long enough to change its overall temperature, and to test if macroscopic changes could be ignited by interfacial changes.

IV Results for pnipam solutions with added surfactants

A Interfacial properties

We have added various amounts of SDS in the pnipam solutions, and focus on concentrations of SDS, c_{sds}, ranging from cmc/300 to cmc/5, where cmc is the critical micelle concentration of SDS, and equal to 8×10^{-3} M.

We then performed experiments similar to those described previously without SDS. The interfacial tension at equilibrium is slightly modified by the surfactants: only smaller values of 2–3 mN m^{-1} at low temperatures for the highest c_{sds} (*i.e.* cmc/5 to cmc/20). At high temperature, we obtain values almost the same as without SDS.

In contrast, it turns out that the addition of SDS has a strong impact on the dynamical properties. For the dilational viscoelasticity and for c_{sds} higher than cmc/50, all the thermoresponsive features are removed. For c_{sds} = cmc/50 and c_{sds} = cmc/100, slight dependence on the temperature is found. Fig. 8 shows the results for cmc/50: only a small increase of E_i is recovered close to T_2. It is then only for c_{sds} = cmc/200 and below that the interface is found unaffected, and the pure pnipam behavior is recovered. For comparisons, at $T = 39$ °C, the elastic moduli are $E_i = 21$ mN m^{-1} and 35.3 mN m^{-1} respectively for c_{sds} = cmc/100 and c_{sds} = cmc/200. Also, note that adding a small amount of SDS at a concentration cmc/100 has typically the same effect as dividing the polymer concentration c_p by 10 ($c_p = 1$ g L^{-1}).

The same trends are actually observed for the shear viscoelasticity (Fig. 9). The addition of SDS at concentrations higher than cmc/50 annihilates all the thermal reactivity. As for dilational results, only a small reminiscence of the temperature

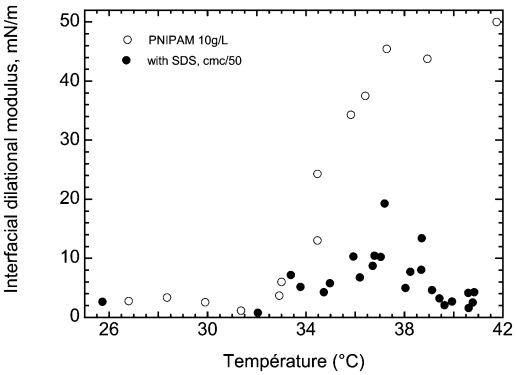

Fig. 8 Effect of the addition of SDS, with a concentration of cmc/50, on the dilational modulus E_i.

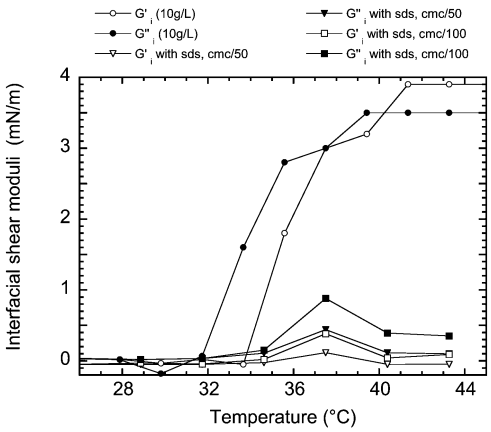

Fig. 9 Effect of the addition of SDS, with concentrations of cmc/50 and cmc/100, on the interfacial shear moduli. Data are collected for a given frequency and strain: $f = 0.2$ Hz and $\tau = 1\%$.

dependence, close to T_3, is detected for SDS concentrations of cmc/50, while it is only slightly higher for cmc/100 (and never with an elastic response) (Fig. 9). It requires a concentration of cmc/200 to reach viscoelastic moduli higher than for $c_p = 1$ g L^{-1} (Fig. 5), and approaching those at $c_p = 10$ g L^{-1}.

Note that, for all the rheological measurements, the effect of the surfactant is smooth: the shift from the regime where SDS has no impact to the one where SDS has removed all the thermal responsivity corresponds to c_{sds} varying between cmc/200 and cmc/50; for further comparisons, we select an intermediate threshold value, $c_t \sim$ cmc/100, to describe this concentration range.

Lastly, adding a cationic surfactant, as tetradecyltrimethylamonium bromide (TTAB), leads to the precipitation of a macroscopic gel-like blob floating in the solution, preventing any further experiments. Experiments with either nonionic surfactants or nanoparticles are under progress.

B Bulk, foaming and stability

Quantitatively, as it could be expected, adding surfactants helps both in foaming the mixed solution, and in stabilizing the

foams produced, but this depends strongly on the amount of added SDS. Our results show that for $c_{sds} < cmc/50$, there is no impact on the foaming and foam stability, which remain as for the ones of pure pnipam solution in Fig. 7, with large holes occurring all through the foam (whatever the solution temperature). As the SDS concentration is further increased, the films between bubbles become more stable, and less macroscopic holes are formed. Consequently, the typical timescales for the decrease of the liquid fraction are of the order of hundreds of seconds. Finally, a good foaming and a subsequent stability of foams actually require a minimal concentration of SDS of cmc/10. On the most stable foams, with large amount of added SDS, various tests do not show any reaction to temperature.

V Discussion

In this section, we come back to some of the results presented above, and compare them to previous works on pnipam solutions and on the pnipam interfacial microstructure and rheology.

The first remark is that all the critical temperatures found in these new experiments are equal: $T_1 = T_2 = T_3 = T_4$ within typically 1 °C, and can also be identified to the known reported values of the transition in the bulk T_c.[17–19,24] Thus, whatever the interfacial or bulk properties, dynamical or static, one can ascribe a same single critical temperature to pnipam. For the interfacial rheology of pure solutions, our results show that it is possible to widely tune the viscoelastic moduli with T: this allows to shift from "fluid-like" interfaces (with basically no viscoelasticity) below T_c, to "solid-like" interfaces above T_c. Note though that the transition is not too sharp in temperature, so that any viscoelastic values can be found by fine tuning of T or c_p.

These results are consistent with previous works on interfacial rheology, in particular with recent interfacial shear results[27] obtained with a different method (a magnetic needle device[27]). Quantitative agreements are actually found, as well as on the effect of the heating protocol. Other previous works on pnipam interfaces mostly dealt with the determination of the static interfacial structures. The understanding obtained from these microscopic structural studies is indeed consistent with the dynamical macroscopic properties measured here. The highly viscoelastic regime found here at high temperature fits well with the highly entangled thick layer of polymer, deduced from scattering methods.[24] An important point of our study is that it shows, for the first time, that not only the shear rheology, but also the dilational rheology has a drastic change at T_c. This implements the previous works, and finally provides a more complete description of pnipam-covered interfaces.

Concerning these high temperature interfaces, we also bring new understanding by the oscillations at constant shear rate. The crossover frequency F_c gives a typical timescale of the relaxation processes in the layer, separating the elastic and viscous regimes. At high enough shear rates (inset of Fig. 6), we observed a regime fully driven by the applied shear which is the origin of the stress relaxation: $F_c \approx \dot{\gamma}$ (see eqn (1)). Interestingly, as $\dot{\gamma}$ decreases, there is a cutoff, and the relaxation processes become independent of the shear rate: F_c tends to F_{c0}. The layer can thus by itself relax stress, and has its own intrinsic dynamics. Such behavior is typical of an aging system, and all the features reported in Fig. 6 are encountered in 3D jammed materials like foams, pastes or emulsions. Therefore, the high temperature layer can be considered as a 2D soft glassy system, slowly evolving with time. Our results in Fig. 4 also confirm this glassy state: the interface can also be unjammed by applying a shear, and for large enough strains, yielding occurs. Such a yielding or unjamming both at high strains – or low frequency – can be described by a Deborah number, defined respectively in terms of deformation or time scales, and separating fluid-like to solid-like behavior.[38,39] It is striking to find that all the frameworks measured and developed for 3D systems remain valid for such a thin polymeric layer (even in the value of the exponent β, being 0.8, and not 1 (ref. 38 and 39)). Microscopically, the intrinsic dynamics are most likely related to rearrangements of chains within this out-of-equilibrium layer.

The effect of the addition of surfactant is also surprising: our results demonstrate that a small molecular weight surfactant like SDS can drastically affect the interfacial dynamics of the polymer layer. Though the impact of SDS is gradual with concentration, we can estimate a concentration threshold, c_t, which is of the order of cmc/100. The effect of SDS is detected at high temperature (removing the viscoelastic properties), while at low temperature, the viscoelastic measurements show that the interface is always fluid-like, whatever the amount of added SDS. However, note that finding the same viscoelastic properties does not necessarily mean that the interfacial organization is independent of the presence of SDS.

It is then important to compare to previous structural studies on SDS–pnipam interactions in bulk and at interfaces. It was found that changes in the interfacial organization require that the concentration of SDS is higher than a critical aggregation concentration (CAC), estimated at $c_{sds} = CAC = 9 \pm 1 \times 10^{-4}$ M (ref. 30 and 33) and corresponding to cmc/10. Scattering techniques, scanning the microscopic static organization, showed that it is only above CAC that the polymer layer is progressively disrupted by the surfactants, which displaced the chains from the interface. It turns out that this CAC threshold is also found in the bulk, and at the same value.[18,28] These results, found for $T < T_c$, tend to show that adding SDS can, at the maximum, only remove the polymer from the interface, thus making this interface more and more fluid-like. As it is already fluid-like, without SDS, it is then obvious to detect no effect of SDS.

More interestingly, for $T > T_c$, it is not yet clear if the CAC is also relevant in such a bad solvent situation.[28] Indeed, for $T > T_c$, the influence of SDS in the bulk and at the interface is more complicated,[16,28,29,31,32] and not fully characterized. It is accepted that the addition of SDS leads to the fragmentation of large pnipam aggregates, preventing precipitation, and leading to colloidal particles (or globules) stabilized by the surfactant. But there is no well-defined amount of surfactant required for this effect. Beside fixed critical values, it has also been reported that the mass ratio R (R = surfactant mass/polymer mass) can be a relevant parameter.[29] Quantitatively, in ref. 16, SDS helps to solubilize globules and to prevent aggregation as soon as its

concentration $c_{sds} > 10$ μM, while R needs to be bigger than 0.05 in ref. 29, for this solubilization effect. Despite these uncertainties for the minimal amount of SDS required, the phase made of SDS-stabilized colloidal particle is expected to remain the same for a large range of SDS concentrations. It is only when the amount of SDS typically approaches the CAC that a different organization is found in the bulk (necklace-like structure, resulting from further solubilization of pnipam). In terms of the interfacial structure, it has been proposed that the interfacial layer is made of adsorbed colloidal particles; but this was measured only for large quantities of SDS ($R > 0.2$). In fact, there are no systematic studies at the interface, as a function of the SDS, in the bad solvent regime.

In comparison with these previous works, for $T > T_c$, the value $c_t \sim$ cmc/100 $= 8 \times 10^{-5}$ M found here by the rheological measurements turns out to be a new feature and a never reported threshold: it is both well below the reported CAC, well above 10 μM, and corresponds to $R = 2.5 \times 10^{-3}$, thus far from the range $R \approx 0.05$ to 0.1. We can then figure out that, when in a bad solvent and depending on c_{sds}, there is a different partitioning of the pnipam chains between the interfacial layer and the colloidal particles. For $c_{sds} < c_t$, the pnipam chains are still mainly precipitated and entangled at the interface leading to the viscoelastic behavior, while for $c_{sds} > c_t$, the pnipam is preferentially collapsed within the colloidal globules. In the last case, the interface must always lose its viscoelasticity, even if the globules are eventually adsorbed (as this does not correspond to an entangled structure at the interface). The transition between the two possible configurations for pnipam in a bad solvent (adsorption at the interface *vs.* aggregation in globules in the bulk) is progressively driven by the amount of SDS: increasing the concentration of SDS allows stabilization of more and more globules in the bulk. In that respect, the threshold value c_t can be considered as a new CAC, valid in the high temperature (bad solvent) regime.

After the discussion of all the purely interfacial results, we can consider the macroscopic scale and the observations made on foams. With pure pnipam solutions, we have found that the solutions can foam only with high energy input, and only initially wet foams can be produced. Moreover, all the resulting foams are always unstable (Fig. 7), and always vanish with large holes occurring everywhere in the foam. This behavior is typical of bubble coalescence induced by too low or non-uniform disjoining pressures produced by the interfaces of the films separating the bubbles.[1,3] A previous work using a technique of suspended films showed that one film can be stable, with only pnipam adsorbed on each film interfaces.[41] In this study, for the low capillary suction investigated ($P_c = 50$ Pa), the equilibrium thickness was of the order of 100 nm.[41] This is consistent with our results on the foaming of the solution: there are indeed some repulsive forces to avoid instantaneous coalescence of bubbles, and to produce wet foams (corresponding to low capillary suction on the films, such as tens of Pa). But within our draining foams, the range of capillary suction from the liquid channels (known as 'Plateau borders') on the films rapidly increases up to hundreds of Pa: this is both due to a liquid fraction decreasing down to a few percents (Fig. 7), and to typical Plateau border radii reaching typically tens of microns (for the initial bubble size used here).[1–4] The observed collapse of the foams shows that the repulsion between the interfaces of the films separating bubbles can only support low capillary suctions, but cannot counterbalance the high capillary suction occurring as the foams drain. This is most likely due to the nature of the repulsive forces providing the disjoining pressure, and also to their spatial uniformity. In ref. 41, it is proposed that the main origin of the repulsive interaction is due to steric effects between loops of pnipam chains floating in the film. Based on the structural studies,[30,33] it is known that, below T_c, the polymer is randomly adsorbed by small chain portions, while a large part of the chains remain in loops in the bulk. Though it can lead to a surface tension decrease (Fig. 1), this configuration might not give uniform and large interfacial coverage. As well, these dangling chains can rearrange and flow as confinement occurs while the film thins down. In that respect, under thinning, there might be parts of the interstitial film between two bubbles which eventually contain no polymers and can therefore be very fragile, as the repulsive forces locally vanish. Thus, we believe that – despite pnipam chains adsorbing rapidly at the interfaces and inducing repulsive forces and positive disjoining pressures when two bubbles come in contact – the major limits for a complete stabilization of the interstitial films are both the spatial uniformity of the repulsive forces, and the low range of these forces (low disjoining pressures) created between the two interfaces.

Following this picture, one could expect that at high temperature, above T_c, the film stability could be higher as a dense polymer layer covers the whole surface of the bubbles. However, one must also consider here the effect of the experimental protocol. A uniform and dense interfacial coverage is found only if the temperature is gradually increased on a same already-covered interface. In the case where the interface is initially created at high T, the smaller values of the viscoelastic moduli found here, and in ref. 27, imply a more heterogeneous spatial adsorption, with the presence of confined aggregates, unfortunately leading both to unstable films and foams.

Adding a surfactant could have been a route to stabilize the foams: we have shown here that SDS actually helps to stabilize such foams, as the surfactant creates a uniform distribution of charges on the interface, leading to efficient repulsive forces between faces of the bubbles. But our results show that the amount of SDS required to stabilize the foam (∼cmc/10) also implies that the interfaces have lost their high viscoelasticity (as soon as $c_{sds} > c_t \sim$ cmc/100).

Ideally, to obtain a stable pnipam foam without adding surfactants, each bubble should be prepared independently below T_c and gradually heated above T_c to obtain a dense viscoelastic interface for each of them; then bubbles could be put in contact and coalescence would then probably be prevented. But this route, based on a parallel preparation and heating of independent bubbles, remains not feasible. More realistically, increasing the pnipam concentration above 10 g L^{-1} has to be tested, as well as reducing the bubble diameters (towards sub-millimeter diameter) so that the contact film area and the probability of film rupture are reduced.

VI Conclusions and perspectives

These new results implement previous ones on pnipam-covered interfaces on four different aspects. First, we report an original quantitative study of interfacial dilational rheology as a function of T. Importantly, these dilational measurements are performed together with interfacial shear rheology and on the same samples. Therefore, clean comparisons can be made between dilatation and shear, as well as between dynamical and structural properties. Without added surfactants, it turns out that, for dynamical properties and both types of dynamical solicitations, a critical temperature T_c is well defined, separating different viscoelastic regimes, as for the structural studies. These results have then allowed us to draw some clear correlation between the scattering techniques, which investigate the microscopic structure of the interfacial layers to the macroscopic interfacial viscoelasticity.

Secondly, by using an original type of oscillatory shear solicitation (at constant shear rate), we have evidenced the glassy nature of the high temperature interfacial layers, which has its own intrinsic slow relaxation.

Thirdly, we have investigated for the first time the effect of the addition of a surfactant on this interfacial viscoelasticity. We have found clear evidence that already minute amounts of surfactant are sufficient to remove the thermal reactivity of the interfacial viscoelasticity: the high viscoelasticity measured for $T > T_c$ vanishes as the SDS removes pnipam from the interface towards colloidal globules in the bulk. Quantitatively, we show here that the surfactant concentration threshold $c_t \sim$ cmc/100 for removing thermal responsivity and interfacial viscoelasticity at $T > T_c$ is at least 10 times smaller than the already reported threshold (CAC = cmc/10), which is a criterion finally only valid for $T < T_c$.

Lastly, we report for the first time the results of foaming of pnipam solutions, with and without surfactant. By comparing the interfacial and foam studies, we have been able to determine that the surfactant concentration threshold for removing the thermal reactivity of the interface is also well below the one required to stabilize a foam.

From a more general point of view, these results are another piece of clear evidence that transposing or extrapolating results obtained at the scale of a single interface to the one of a single film of liquid (two interacting interfaces) or to the one of a foam remain tricky. Here we have found that *a priori* negligible changes of formulation (like adding traces of surfactant) can already provide drastic changes, in particular in terms of interfacial rheological properties. As well, the stability of a single film[41] does not necessarily mean the stability of a foam. Also, the role of the experimental and heating protocol is also crucial: the interfacial configuration deduced from measurements on a single interface and the one inside a foam can be different, as they are not necessarily prepared following the same paths. In contrast, it is interesting to point out that there are good correlations existing between the polymer–surfactant associations in bulk and the interfacial properties. As often observed, advanced investigations of the interfaces (beyond simple surface tension measurements) can actually reveal changes of configuration or properties in the bulk. For pnipam without surfactant, structural microscopic studies of the interfaces were already consistent with results in the bulk: we demonstrate here that the macroscopic dynamical properties are also reflecting the changes of solvent quality for pnipam with temperature. With surfactant, it turns out that associations occurring in bulk and competition between the bulk and interface are also revealed through interfacial rheological features.

Beside using pnipam in foams, using such a system with a 2D rheology reversibly responsive to temperature is interesting for many dynamical processes involving free liquid interfaces. As already stated, dynamical situations leading to out-of-equilibrium deformation of interfaces could be investigated with such a responsive solution, presenting the advantages of having any interfacial viscoelasticity set by the external conditions. Therefore, a pnipam solution can be seen as a simple model system allowing us to tune reversibly the interfacial dynamical properties, both in shear and dilatation. The rate of heating, the polymer concentration, and the addition of surfactant are parameters which control the final state and viscoelasticity, and can then provide a controlled tailoring of liquid interfaces.

Acknowledgements

This work has been supported by ANR grant "NewFoam"-Blan-07-340. The authors thank L. T. Lee for discussions and for providing samples for preliminary tests.

References

1 R. K. Prud'homme and S. A. Khan, *Foams: Theory, Measurements, and Applications*, Marcel Dekker Inc., New York, 1997.
2 A. Saint-Jalmes, D. J. Durian and D. A. Weitz, *"Foams", in Kirk-Othmer Encyclopedia of Chemical Technology*, 5th edn, 2005.
3 I. Cantat, S. Cohen-Addad, F. Elias, F. Graner, R. Höhler, O. Pitois, F. Rouyer and A. Saint-Jalmes, *Les mousses, structure et dynamique*, Belin, Paris, 2010.
4 A. Saint-Jalmes, *Soft Matter*, 2006, **2**, 836.
5 S. Tcholakova, N. D. Denkov and A. Lips, *Phys. Chem. Chem. Phys.*, 2007, **10**, 1608.
6 B. Scheid, J. Delacotte, B. Dollet, E. Rio, F. Restagno, E. A. VanNierop, I. Cantat, D. Langevin and H. A. Stone, *Europhys. Lett.*, 2010, **90**, 24002.
7 A. Q. Shen, B. Gleason, G. H. McKinley and H. A. Stone, *Phys. Fluids*, 2002, **14**, 4055.
8 N. D. Denkov, V. Subramanian, D. Gurovich and A. Lips, *Colloids Surf., A*, 2005, **263**, 129.
9 C. D. Bain, *Adv. Colloid Interface Sci.*, 2008, **144**, 4.
10 C. J. W. Breward, R. C. Dalton, P. D. Dalton, P. D. Howell and J. R. Ockendon, *Chem. Eng. Sci.*, 2001, **56**, 2867.
11 E. Dickinson, *Colloids Surf., B*, 1999, **15**, 161.
12 P. J. Wilde, *Curr. Opin. Colloid Interface Sci.*, 2000, **5**, 176.

13 G. J. Fleer, M. A. Cohen Stuart, J. M. H. M. Scheutjens, T. Cosgrove and B. Vincent, *Polymers at Interfaces*, Chapman and Hall, London, 1993.
14 G. B. Bantchev and D. K. Schwartz, *Langmuir*, 2003, **19**, 2673.
15 M. Heskins and J. Guillet, *J. Macromol. Sci., Part A*, 1968, **2**, 1441.
16 J. Ricka, M. Meewes, R. Nyffenegger and T. Binkert, *Phys. Rev. Lett.*, 1990, **65**, 657.
17 H. G. Schild and D. A. Tirell, *Langmuir*, 1991, **7**, 665.
18 H. G. Schild, *Prog. Polym. Sci.*, 1992, **17**, 163.
19 M. Kawagushi, W. Saito and T. Kato, *Macromolecules*, 1994, **27**, 5882.
20 M. Kawagushi, Y. I. Hirose and T. Kato, *Langmuir*, 1996, **12**, 3523.
21 J. Zhang and R. Pelton, *Langmuir*, 1996, **12**, 2611.
22 J. Zhang and R. Pelton, *Langmuir*, 1999, **15**, 8032.
23 J. Zhang and R. Pelton, *Colloids Surf., A*, 1999, **156**, 111.
24 L. T. Lee, B. Jean and A. Menelle, *Langmuir*, 1999, **15**, 3267.
25 Q. R. Huang and C. H. Wang, *Langmuir*, 1999, **15**, 634.
26 B. A. Noskov, A. V. Akentiev, A. Y. Bilibin, D. O. Grigoriev, G. Loglio, I. M. Zorin and R. Miller, *Langmuir*, 2004, **20**, 9669.
27 C. Monteux, R. Mangeret, G. Laibe, E. Freyssingas, V. Bergeron and G. Fuller, *Macromolecules*, 2006, **39**, 3408.
28 R. Walter, J. Ricka, C. Quellet, R. Nyffenegger and T. Binkert, *Macromolecules*, 1996, **29**, 4019.
29 L. T. Lee and B. Cabane, *Macromolecules*, 1997, **30**, 6559.
30 B. Jean, L. T. Lee and B. Cabane, *Langmuir*, 1999, **15**, 7585.
31 R. M. Richardson, R. Pelton, T. Cosgrove and J. Zhang, *Macromolecules*, 2000, **33**, 6269.
32 B. Jean, PhD thesis, Universite Paris 6, Paris, 2000.
33 B. Jean and L. T. Lee, *J. Phys. Chem. B*, 2005, **109**, 5162.
34 J. Benjamins, A. Cagna and E. H. Lucassen-Reynders, *Colloids Surf., A*, 1996, **114**, 245.
35 P. Erni, P. Fischer, P. Windhab, E. J. Kusnezov, V. Stettin and H. Lauger, *J. Opt. Soc. Am. Rev. Sci. Instrum.*, 2003, **74**, 4916.
36 P. Erni, P. Fischer, P. Heyer, P. Windhab, E. J. Kusnezov and H. Lauger, *Prog. Colloid Polym. Sci.*, 2004, **129**, 16.
37 K. Feitosa, S. Marze, A. Saint-Jalmes and D. J. Durian, *J. Phys.: Condens. Matter*, 2005, **17**, 6301.
38 H. M. Wyss, K. Miyazaki, J. Mattsson, Z. Hu, D. Reichmann and D. A. Weitz, *Phys. Rev. Lett.*, 2007, **98**, 238303.
39 S. Marze, R. M. Guillermic and A. Saint-Jalmes, *Soft Matter*, 2009, **5**, 1937.
40 R. Krishnaswamy, S. Majumdar and A. K. Sood, *Langmuir*, 2007, **23**, 12951.
41 B. Jean, L. T. Lee, B. Cabanne and V. Bergeron, *Langmuir*, 2009, **25**, 3966.